

Challenges and Opportunities of Data Driven Advance Classification for Hard Rock TBM excavations

Georg H. Erharter^{1a*}, Paul Unterlaß^{2a}, Nedim Radončić³, Thomas Marcher², Jamal Rostami⁴

1) Norwegian Geotechnical Institute, Sandakerveien 140, Oslo, Norway

2) Institute of Rock Mechanics and Tunnelling, Graz University of Technology, Rechbauerstraße 12, Graz, Austria

3) iC Consulente ZT GmbH, Schönbrunnerstraße 12, Vienna, Austria

4) Colorado School of Mines, 1500 Illinois St, Golden, Colorado, United States of America

* correspondence: georg.erharter@ngi.no

Preprint statement: This manuscript is a non-peer reviewed preprint submitted to EarthArXiv.

Highlights

- TBM operational data is a more objective basis for tunnel advance classification
- TBM data analysis can be challenging and requires transparent, computational tools
- Generative adversarial networks are used to provide open, synthetic TBM data
- Recommendations for data driven TBM advance classification are given

Abstract

Excavation with tunnel Boring Machines (TBMs) is a widely used method of tunneling in all ground types including soil and rock today. The paper addresses the shift from traditional subjective methods to data-driven approaches for advance classification of TBMs in hard rock tunnel excavation. By leveraging continuous TBM operational data, these methodologies offer more objective, transparent, continuous and reproducible assessments of excavation conditions. The challenges include the need for sophisticated computational tools to interpret complex interactions between rock mass, TBM machinery, and logistics that are sensitive to the whole data processing pipeline. This contribution provides consistent, step-by-step recommendations for how to efficiently process TBM operational data. It furthermore provides the community with 3 open TBM operational datasets that can be used for benchmarks and educational purposes related to TBM data processing. To overcome data confidentiality issues, the datasets are synthetic and were generated with generative adversarial networks (GANs) – a method of artificial intelligence -, that are trained on real TBM operational data. It is thus ensured that the data on the one hand looks like real data, but has no direct relationship to real construction sites. This study highlights the potential of data-driven techniques to improve TBM tunnelling efficiency, while addressing key technical challenges.

^a These authors contributed equally to this work.

30 **Keywords:** TBM tunnelling, Hard Rock TBM, TBM performance analysis, advance classification, data preprocessing,
31 generative adversarial networks

32 1. Introduction

33 Excavation by tunnel boring machine (TBM) has become the method of choice for driving longer tunnels in mostly
34 homogeneous rock mass conditions (Maidl et al. 2008). As in all tunnel excavations, TBM tunnelling requires continuous
35 characterization and classification of the encountered system behavior (i.e. the behavior of the rock mass in combination
36 with the chosen construction and excavation measures) (ÖGG 2023). This approach is necessary to i) react to variable
37 ground conditions with respect to the TBM operation (e.g., careful advance in adverse ground conditions), ii) adjust the
38 tunnel support according to the encountered ground conditions (e.g. using standard vs. heavy ground support) and iii)
39 have a more consistent basis for compensation of the contractor depending on the established measurement and payment
40 in various ground classes within the overall contractual framework. The usual way of acquiring these system behavior
41 classifications is to follow geomechanical design guidelines, as for example given by ÖGG (2023), or to use one of many
42 existing rock mass classification schemes (Erharter et al. 2024) in combination with the project specific contractual
43 framework.

44 These “classical” approaches towards system behavior classification suffer from the shortcomings of subjective
45 perceptions of onsite personal which need to assess the current state of the excavation using their natural sensory systems:
46 see, smell, touch. While this is less of a challenge in conventional drill and blast tunnelling due to unconfined access to the
47 tunnel face and -walls, this approach is particularly problematic in TBM tunnelling where the observability of the rock
48 mass conditions is largely obstructed due to the TBM machinery, thus rendering sensory perceptions even more unreliable.
49 Additionally, “classical” excavation condition assessments, that are mostly done once per day, are in conflict with high
50 performance TBM excavation for two more reasons: i) high excavation performance (up to over 30 meters per day) is
51 achievable today, but physical inspection visits to the cutterhead are, in principle, time consuming and reduce excavation
52 performance even though they are necessary to keep the TBM running, ii) large observational gaps occur if a high
53 excavation performance is achieved but the excavation conditions are only characterized once per day.

54 To alleviate the downsides of classical system behavior determination, increasing focus is directed onto deriving the system
55 behavior from the TBM operational data which modern TBMs often record on 1 Hz or sample per second frequency. The
56 recorded TBM operational parameters are a function of: i) the encountered rock mass conditions (e.g. intact rock strength,
57 lithology, discontinuity network, in situ stresses), ii) the TBM machinery (e.g. thrusting power, cutterhead geometry, wear
58 state of cutters) and iii) the working processes and logistics (e.g. driving style of the TBM operator, maintenance
59 procedures) (Thuro 2002); (Figure 1).

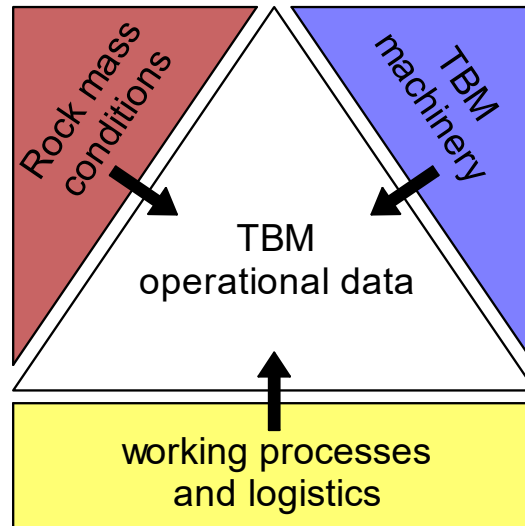


Figure 1: Main influences on the TBM operational data (modified after Thuro (2002)).

This combination of different influences makes it challenging to interpret individual signals (e.g., if one is only interested in the rock mass conditions) and one must be aware that interpretation of this data is affected by uncertainty. Nevertheless, the combination of all these different operational influences makes the TBM data well suited for identifying the system behavior as a whole. Advance classification based on TBM operational data has the following advantages over classical classification: i) data-driven classifications are comprehensible and reproducible and not based on subjective engineering judgement; ii) the TBM operational data is recorded in any case and thus the excavation performance is not disrupted by the face inspection and classification effort; iii) the TBM operational data provides a continuous and uninterrupted record of the excavation conditions and thus allows for continuous advance classification. It must be noted, however, that TBM advance classification based on analysis of operational data is not necessarily fully objective, as also the data driven classification process requires manual interventions.

Recognizing these advantages, recent studies looked into data-driven advance classification, also utilizing machine learning technology (e.g. Erharter and Marcher (2020); Liu et al. (2020); Liu et al. (2021); Xue et al. (2023)). Early indications of the possibility to use the TBM operational parameters to identify the ground conditions and to recognize the possibility of high ground convergence in weaker rock masses based on cutterhead torque were in the early 2000's when some of the shielded machines working in weak rock masses had to deal with long delays due to machine entrapment. These studies showed that low torque reading combined with high thrust was a good indicator of weak formations ahead alerting operators to the possibility of high ground convergence, which could be avoided by faster tunneling in related formations (Farrokh and Rostami 2008, 2009). While these approaches pushed the early research front, the recently published Austrian contractual standard ÖNORM B 2203-2: "Underground Works – Works Contract – Part 2: Continuous Driving" (ÖNORM B 2203-2:2023, 2023), seems to be the first attempt towards implementing data-driven advance classification in engineering practice. The data-driven advance classification scheme of the ÖNORM B 2203-2 is based on the "torque ratio" which is a parameter computed from TBM operational data, that was first introduced by Radoncic et al. (2014) in the course of the Koralm base tunnel project. Since then, the parameter was incorporated into a contractual framework

85 that was developed since 2016 with intermediate reports provided by Bach et al. (2018), Radončić et al. (2019) and Holzer
86 et al. (2021). The torque ratio is used for demonstration in this paper, although other parameters for advance classification
87 are possible as well.

88 This new standard is a step towards more comprehensible and transparent TBM advance classification. However, new
89 systems like this come along with challenges and data driven advance classification requires that the geotechnical engineer
90 onsite has to deal with unprecedented data analyses problems outside of their usual domain of expertise. This paper
91 therefore follows two main objectives: i) it provides extended explanations and guidance on the application of data-driven
92 TBM advance classification. Extended elaborations as presented herein go beyond the practical framework of a contractual
93 standard and extend on scientific literature about TBM data classification that was given above. ii) As an additional aid for
94 practitioners, TBM operational data is provided in the data availability section of this paper, including examples for how to
95 compute the torque ratio based advance classification using Python. To avoid the problem of confidentiality that comes
96 with real datasets, the provided data was synthesized in a novel way using artificial neural networks that were trained to
97 mimic patterns of real TBM operational data while creating original and new data that is unrelated to real construction
98 sites (Unterlass et al. 2023).

99 Methodological explanations on how the torque ratio is computed and how realistic TBM operational data for three
100 construction sites is synthesized are provided in section 2. A workflow for processing TBM operational data for advance
101 classification is then presented in section 3. The data processing is discussed in section 4 and the paper finishes with a
102 conclusion and recommendations for the TBM operational data based advance classification in practice in section 5.
103 Synthetic TBM datasets and Python codes are provided through a link to a Github repository in the paper's data availability
104 section. References to files in the code repository are given at the end of relevant paragraphs in that form: "(see Github
105 repository: FOLDER, FILENAME, FILETYPE)".

106 2. Methodology

107 2.1. Computation of torque ratio

108 The definition of the torque ratio has been introduced due to the need for a dimensionless variable allowing insight into
109 the basic coupling between the main operational parameters of a hard rock TBM. Required input variables are a TBM's
110 penetration rate [mm/rot] (i.e. advance length per rotation of the cutterhead), cutterhead thrust [kN], cutterhead torque
111 [kNm] and disc cutter layout on the cutterhead. They are coupled by the simple fact that the cutterhead is constantly
112 rotating, and therefore the resulting disc cutters' cutting force is acting in both axial (against the direction of the advance)
113 and tangential (against the cutterhead rotation) direction. The cutterhead thrust is the sum of all normal forces of the
114 cutters, and the cutterhead torque is the sum of the moment caused by all cutters as a result of the rolling force. The ratio
115 between the measured cutterhead torque and the theoretical cutterhead torque gives an indication whether or not all
116 disc cutters are in contact with the face. If the measured torque is substantially different than the computed one, it can
117 indicate that either not all cutters are in contact with the face (which can point to a partial face failure / over-break from

118 the face), or an additional frictional resistance is mobilized (for instance: by having debris and fragments between the
119 cutterhead and the face).

120 The torque applied on the cutterhead is either directly measured and recorded in the TBM operational data or can be
121 calculated from i) the recorded electric current and/or power applied to the electric drive of the cutterhead to which it is
122 linearly coupled or ii) from the pressure and flow of the lines for a hydraulic drive system. The exerted torque (M) is given
123 by dividing the power (P) with the rotational speed of the cutterhead (ω) (eq. 1):

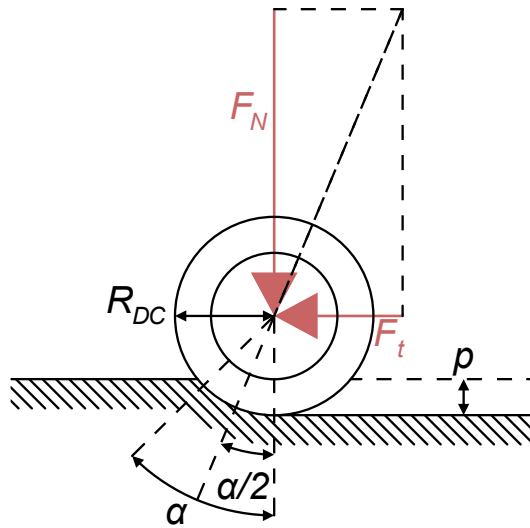
$$M = \frac{P}{\omega} \quad \text{eq. 1}$$

124

125 The theoretical torque is computed applying the relationships published by Rostami (1997, 2013) or Rostami and Ozdemir
126 (1993) in their simplified form for calculation of normal and rolling forces. The cutting angle (α), defining the theoretical
127 contact area between the rock and the disc cutter, is a function of penetration (p) and the disc cutter radius (R_{DC}) as in
128 eq. 2. The general setting of the disc cutter cutting condition is shown in Figure 2:

$$\alpha = \arccos\left(\frac{R_{DC} - p}{R_{DC}}\right) \quad \text{eq. 2}$$

129



130

131

Figure 2: Longitudinal section of the disc cutter in operation.

132 The applied disc cutter thrust (F_N) is determined by dividing the total cutterhead thrust (F_{CH}) by the number of installed
133 cutters (n_{disk}) (eq. 3):

$$F_N = \frac{F_{CH}}{n_{disk}} \quad \text{eq. 3}$$

134

135 It is assumed that the cutter force resultant is bisecting the contact area symmetrically, thus allowing calculation of the
136 tangential (rolling) force component (F_t) from F_N and α (eq. 4):

$$F_t = \tan\left(\frac{\alpha}{2}\right) * F_N \quad \text{eq. 4}$$

137

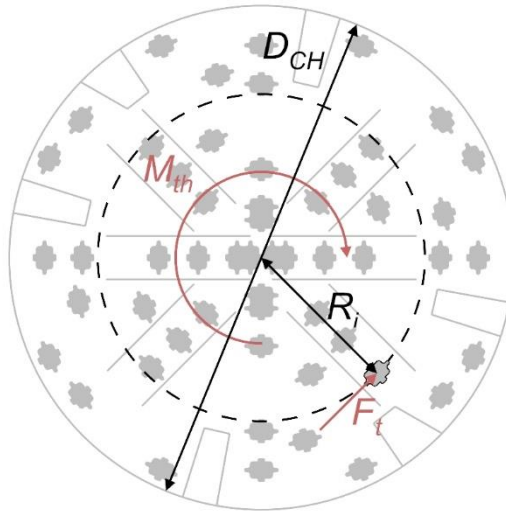
138 The theoretical torque (M_{th}) is then obtained by summing up the product of the individual cutters' tangential forces (F_{ti})
139 with the respective distance to the cutterhead center (R_i) (eq. 5). Alternatively, M_{th} can be approximated with a simplified
140 equation that includes the cutterhead diameter (D_{CH}) (eq. 6).

$$M_{th} = \sum_{i=1}^n F_{ti} * R_i \quad \text{eq. 5}$$

$$M_{th} \sim 0.3 * F_t * n_{disc} * D_{CH} \quad \text{eq. 6}$$

141

142 The corresponding geometrical relationship is presented in Figure 3.



143

144 *Figure 3: Theoretical cutterhead torque and the disc cutter layout on the cutterhead.*

145 The torque ratio (TR) is finally determined as the ratio between the real, recorded cutterhead torque M and the theoretical
146 torque M_{th} under consideration of the frictional loss M_0 (torque required to overcome the internal machine friction and
147 start the cutterhead rotations) (eq. 7):

$$TR = \frac{M}{M_{th} + M_0} \quad \text{eq. 7}$$

148

149 The value of M_0 has been found to equal approximately 250 kNm on large diameter machines ($\emptyset \sim 10$ m) but it is
150 recommended to determine it from the machine data at the beginning of strokes following longer maintenance shifts

151 where the cutterhead was not in contact with the tunnel face. In other words, M_0 is the torque used to rotate the
152 cutterhead when it is not engaged with the face (at zero advance force).

153 The presented relationship has been investigated on different international projects, and it was observed that the
154 relationship is in good accordance with the encountered system behavior for all TBM types with a hard rock cutterhead
155 (Bach et al. 2018). Published examples where different parameters of TBM operational data are plotted in comparison to
156 engineering geological and geotechnical longitudinal profiles can be, for example, found in figure 4 of Radoncic et al.
157 (2014), figure 5 in Reinhold et al. (2017) or figure 5 in Heikal et al. (2021). (see Github repository: src, DATA_XX_library.py,
158 Python file)

159 2.1.1. TBM specific considerations

160 The calculation of the cutterhead thrust is machine type specific and therefore thorough consideration of the entire system
161 is required. In case of double-shield TBMs, the main thrust cylinders are located between the front and the gripper shield.
162 The measured thrust contains the friction of the front shield and the net cutterhead thrust, consequently the shield friction
163 must be regularly determined through test strokes. Additional information on the rock mass loading of the shield is
164 presented by analyzing the forces required to move the gripper shield during regripping, therefore giving direct
165 information on possible presence of debris in the annular gap and/or onset of squeezing pressure building up (Hasanpour
166 et al. 2014; Hasanpour et al. 2015; Hasanpour et al. 2020).

167 A similar logic applies to gripper TBMs, where the applied thrust equals the sum of the gripper shield friction (if there is
168 one) and the cutterhead thrust. Additional information can be retrieved by measuring the pressure development in the
169 shield segments (if present), therefore receiving direct indication on the interaction between the rock mass extrados and
170 the shield (Unterlass et al. 2022).

171 Single shield TBMs usually have actuated cutterheads and can measure the applied cutterhead thrust directly by
172 monitoring the articulation joint cylinders' hydraulic pressure. The main thrust cylinders act on the entire shield. If these
173 force measurements are used, one must consider that the total thrust is in this case the sum of shield friction, cutterhead
174 thrust and the towing force for the backup trailer. More information on TBM shield friction for all TBM types can be found
175 in Erharter et al. (2023).

176 2.2. Generation of artificial TBM data

177 In geotechnical engineering, confidentiality constrains possibilities for the use of real datasets. To bypass this problem, a
178 generative adversarial network (GAN) based approach of generating artificial TBM operational data was adopted
179 (Goodfellow et al. 2014). In accordance with Unterlass et al. (2023), the generated data is associated with the following
180 dualistic requirements: i) the data must be sufficiently dissimilar from the original data, in order not to create
181 confidentiality issues – i.e. the “demand for originality”; ii) it must show the same patterns and follow the same rules as
182 the original data, in order to be used as if it was from a real TBM data – i.e. the “demand for conformity”.

GANs belong to the group of generative classifiers (Ng and Jordan 2001), and are based on a game theory scenario in which two artificial neural networks compete against each other. The generator network directly produces (artificial) samples from random noise input variables and calculated parameters (i.e. weights). Its adversary, the discriminator, attempts to distinguish between samples taken from the training data (i.e. real data) and samples from the generator (i.e. generated data). The discriminator network outputs a probability value, indicating if the presented sample is real (i.e. taken from the training data) or fake (i.e. generated data). During GAN training, the generator is continuously trying to fool the discriminator by generating ever more realistic data, whereas the discriminator is constantly improving in differentiating between fake and real samples. At convergence, (i.e., the point in training where the generator's samples are indistinguishable from real data), the generator network has successfully learned to accurately reproduce the underlying data distribution, mimicking that of the real-world data.

GAN training and examination of the generated data can be difficult in practice (Goodfellow et al., 2020). However, a previous study (Unterlass et al. 2023) has shown that, particularly Wasserstein GANs (Arjovsky et al. 2017) provide promising results when given the task to specifically generate TBM operational data.

Thorough evaluation is necessary to check whether the requirements placed on the artificial data are met. As proposed in Asre and Anwar (2022), dimensionality reduction algorithms (e.g. t-SNE (van der Maaten and Hinton 2008) and PCA (Pearson 1901)) allow for visual inspection if the artificial data is showing the same patterns and following the same trends as the real data. The demand for originality, validating the preservation of privacy was assessed by using the distance to closest record method (Park et al. 2018). Here, the Euclidean distance between any artificial record and its closest corresponding neighbor from the real data is calculated and evaluated.

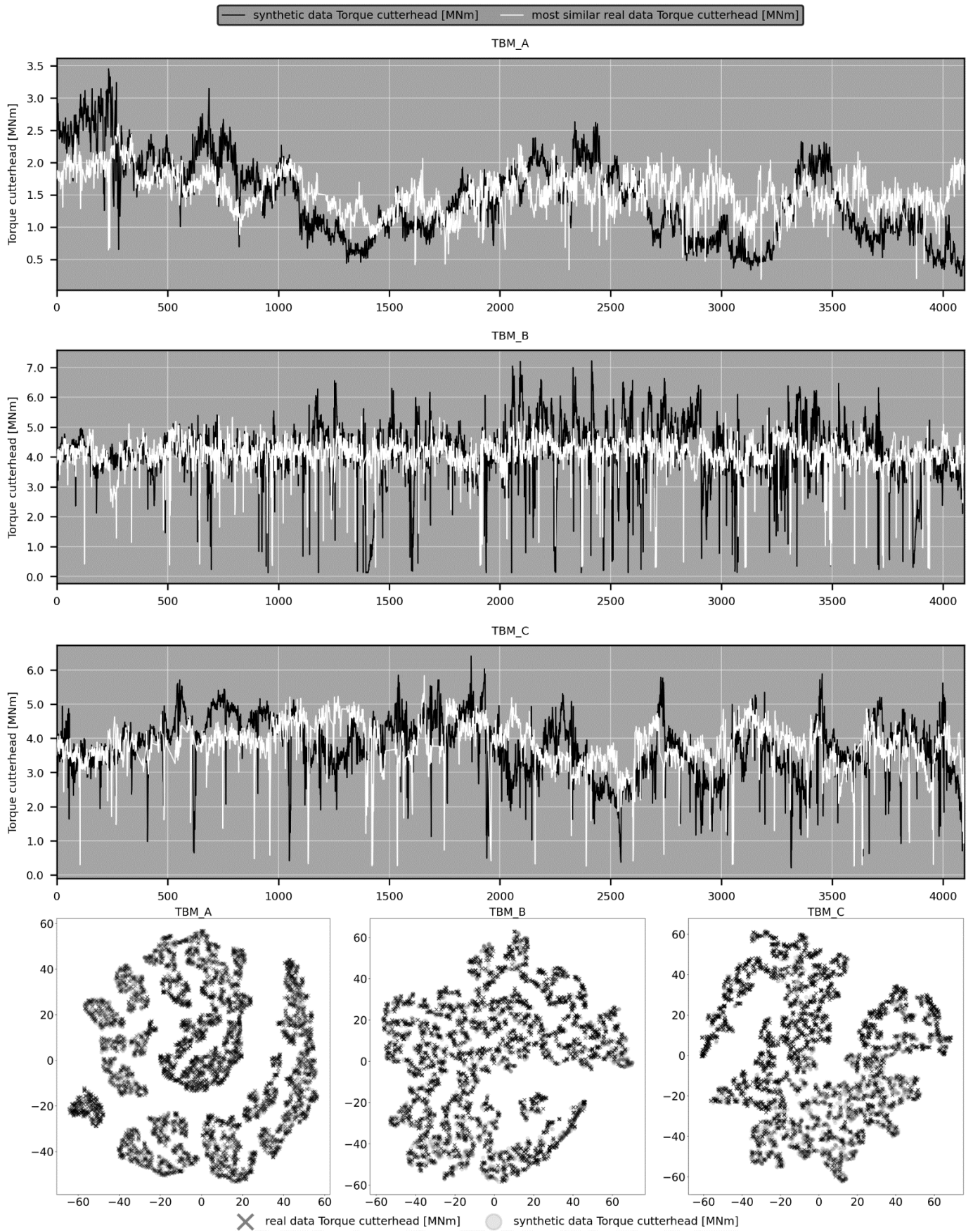
2.2.1. Generated datasets

By applying the Wasserstein-GAN, three sets of artificial but realistic TBM operational data were generated. The generated datasets are based on real TBM operational data from three different construction sites including two gripper TBM excavations (named TBM A and TBM C) and one double shield TBM excavation (named TBM B). (see Github repository: data, "TBM_X_0_synthetic_raw" (replace X with A, B, C for each TBM), parquet files).

By sampling from the trained generator model, i.e. feeding it with random noise, infinite sequences of artificial TBM data can be generated. The data sequences generated in this way have a vector length of 4096 consistent datapoints (i.e. observations) per sequence. This sequence-length is predetermined by the internal architecture of the GAN's artificial neural networks, whereas longer sequence-lengths would significantly increase the demand for computing power. Presenting the GAN model architecture is outside the scope of this paper, but the full source code, including the neural network architecture is given in the src folder of the Github repository in the data availability section of the paper: i.e. the Python scripts starting with "WGAN_". Depending on the average datapoint-spacing in the training data, (e.g. 0.05 m for TBM_A), one sequence of artificial data comprises a continuous section of $spacing * sequence-length$ tunnelmeters (i.e. $0.05 * 4096 = 204.8$ m for TBM_A), however, it must be noted that the tunnel length / chainage for each datapoint was back-calculated based on the artificial penetration rate and a constant number of cutterhead rotations (see below).

217 Figure 4 demonstrates that both the "demand for originality" and the "demand for conformity" are fulfilled in the
218 generated dataset. Rows 1 to 3 show randomly selected artificial sequences of the cutterhead torque [MNm] in the
219 background (black) and the most similar corresponding real TBM data sequence in the foreground (white). Row 4 shows
220 the results of the t-SNE dimensionality reduction for these sequence pairs. From Figure 4 it can be observed that both
221 sequences (real and artificial) plot in the same range, show the same patterns and follow the same trends without being
222 copies.

Data Driven Advance Classification of Hard Rock TBMs
(non-peer reviewed preprint)



223

224 Figure 4: Rows 1-3 show that artificial sequences of the cutterhead torque [MNm] and most similar real TBM training data are sufficiently dissimilar
 225 to count as original (x-axis = n datapoints). Row 4: t-SNE dimensionality reduced representation of real and synthetic TBM data shows that both
 226 datasets exhibit the same underlying structure and data patterns and thus the synthetic data is representative for the real data.

227 The generated data which consists of penetration [mm/rot], total advance force [kN] and cutterhead torque [MNm] is
228 then further post-processed to increase the realism of the datasets (see Github repository: src,
229 "DATA_01_postprocessor.py", Python file). The following steps are applied:

- 230 ▪ The excavated tunnel length is back calculated by cumulative summation of the generated penetration rate divided
231 by a constant number for cutterhead rotations per minute (TBM A: 6 rpm, TBM B: 5 rpm, TBM C: 5 rpm). The tunnel
232 length is rounded to a precision of centimeters (i.e. meters with two decimals) as is often the case in real TBM
233 operational data. Each of the three generated datasets is limited to 1000 meters in total.
- 234 ▪ Stroke numbers are assigned to the datapoints depending on the tunnel length and a constant stroke length of 1.7
235 meters for all datasets is used.
- 236 ▪ After each stroke, a standstill period with a duration between 0.7 to 2 hours is inserted to represent the regripping
237 and support installation process. In the standstill period penetration, total advance force, cutterhead torque and
238 cutterhead rotations are all 0 and the tunnel length and stroke number are kept constant at the last value of the
239 stroke excavation.
- 240 ▪ A time stamp with sequentially increasing time is generated that starts at 01.01.2024 (arbitrarily chosen) for all
241 datasets but has different time frequencies for every dataset: (TBM A: 10 s, TBM B: 1 s, TBM C: 10 s).

242 It needs to be mentioned that the goal of the data synthetization was to create the most realistic TBM operational data in
243 a generic way and not to reproduce any construction site specific data. Values such as the stroke length were therefore
244 taken as the same for all three datasets even though they are not the same in reality. Accordingly, the duration of the
245 standstills was arbitrarily chosen. The realistic, post-processed TBM datasets can be found in the paper's data availability
246 section (see Github repository: data, "TBM_X_1_synthetic_realistic.zip" (replace X with A, B, C for each TBM), zipped .csv
247 files).

248 3. Processing TBM data for advance classification

249 The previous section explained how to compute a parameter for TBM advance classification such as the torque ratio
250 (section 2.1) and how realistic and open TBM operational data was created for exemplary purposes of this study (section
251 2.2). Treating the generated data as real TBM operational data, this section will now elaborate on challenges in the data
252 processing procedure. This procedure is separated into these main steps: i) basic data cleaning/screening, ii) spatial
253 discretization, iii) parameter computation, iv) threshold definition and classification. The sequence of these steps is given
254 based on the authors' experience of what works well for various TBM datasets. However, it must be pointed out that the
255 sequence of the presented main steps, as well as some of the sub-steps, may be changed in principle but their order of
256 execution can have impacts on the final result. For example, the main steps ii) spatial discretization (section 3.2) and iii)
257 parameter computation (section 3.3) may be switched as one could do spatial discretization first and then compute
258 parameters such as the torque ratio from the discretized values. The other way round, where the torque ratio is computed
259 from the non-discretized data and then the computed parameters are discretized with the rest of the data is, however,
260 also possible. The choice for the applied order is use-case specific. The important and imperative thing is, however, to have

261 full transparency over the whole processing pipeline, to avoid conflicts that result from discrepancies that may originate
262 from different processing sequences.

263 If advance conditions are to be classified based on TBM operational data, it is imperative that the processing-procedures,
264 mathematical- or statistical steps and chosen hyperparameters are communicated and agreed upon between all involved
265 parties on site. Even slight deviations from one commonly agreed upon processing pipeline can lead to different advance
266 classifications and thus disputes as will be shown in section 3.5. For improved transparency and traceability, it is
267 recommended to perform all TBM data processing using programming languages such as Python and to store the code on
268 version tracked code repositories agreed upon by both parties. The use of spreadsheet calculation software for this
269 purpose is discouraged as the large amount of data makes it not only excessively laborious, but also prone to errors and a
270 lack of transparency. The Python code for TBM data processing which can be used for the exemplary datasets of this paper
271 and other, real TBM datasets can be found in the paper's data availability section (see Github repository: src,
272 "DATA_02_analyzer.py", Python file).

273 3.1. Basic data cleaning

274 The first step in data processing is to remove standstills/delays/disruptions in the excavation process as the advance
275 classification is usually only based on data that is recorded during excavation work of the TBM. Exceptions may exist, as
276 for example presented in Unterlass et al. (2022) where the data from non-advance periods was used to identify rock loads.
277 As proposed by Zhang et al. (2019) and adopted also by Erharter and Marcher (2020), a datapoint is to be seen as a
278 standstill and removed when either one or several of these parameters are equal to 0: cutterhead torque, advance force,
279 cutterhead rotations, penetration. Depending on the TBM's utilization rate, this step typically heavily reduces the overall
280 number of datapoints. In addition, the majority of the TBM manufacturers provide a Boolean/binary flag variable in their
281 data recording indicating "cutterhead rotation" and "TBM advance". If either of these parameters are flagged as "off", then
282 the related data can be removed.

283 TBM operational data is recorded on a regular (temporal) frequency and the recording of the absolute location of the
284 TBM's cutterhead (or other reference points such as the edge of the front shield) with respect to the tunnel chainage is
285 mostly done with a limited spatial resolution of ca. 1 cm. This results in the problem that TBM operational data typically
286 features multiple recorded datapoints for one specific position in the tunnel and the number of datapoints per location is
287 variable because of different advance speeds. For further analysis, it is, however, required to process the data in a way
288 that there is only one unique datapoint per tunnel position. The number of recorded datapoints with the same position
289 (n_{dp_same}) therefore depends on three parameters (eq. 8): the spatial recording resolution [mm] (r), the advance speed
290 of the TBM [mm/s] (s) and the temporal recording frequency [s] (f).

$$n_{dp_same} = \frac{r}{s * f} \quad eq. 8$$

291 For example, if a TBM advances with a speed of 30 mm/min ($s=0.5$), the temporal recording frequency is 1 datapoint every
292 2 seconds ($f=2$) and the spatial recording resolution is 1 cm ($r=10$), then there will be 10 datapoints recorded for every

293 position in the tunnel. If the advance speed increases to 50 mm / min, then n_{dp_same} will reduce to 6 datapoints with the
294 same position.

295 The proposed solution to this problem is to take the arithmetic mean of all datapoints with the same location and thus
296 create one unique datapoint per location (Erharter and Marcher 2020; Unterlass et al. 2023). This second step of basic
297 data cleaning further reduces the total number of datapoints significantly, although typically not as much as the first step.
298 Using other methods to spatially merge datapoints such as the median instead of the arithmetic mean can be considered,
299 but experience shows that this has no significant impact on the outcome. (see Github repository: data,
300 "TBM_X_2_synthetic_advance.xlsx" (replace X with A, B, C for each TBM), excel files)

301 3.2. Spatial discretization

302 Following initial data cleaning, spatial discretization of the data is required. As, for example, discussed in Erharter and
303 Marcher (2021), an inherent challenge of TBM operational data processing is that the data is regularly distributed in time
304 but not in space, but usually the space dimension is the one of interest when it comes to advance classification. The
305 previous step of merging datapoints with the same location in the tunnel lessens the problem to a certain extent but still
306 does so in a spatially inhomogeneous manner and makes the data analyses vulnerable to the spatial resolution of the TBM
307 data recording. It is thus recommended to systematically discretize the data spatially by i) either spatially interpolating and
308 resampling the data with a defined datapoint spacing along the tunnel length or ii) statistically aggregating (i.e. taking the
309 arithmetic mean or median of) the data in discrete distance steps or intervals along the tunnel. While the former was, for
310 example, shown in Erharter and Marcher (2021), the latter is suggested by the ÖNORM B 2203-2 (ÖNORM B 2203-2:2023,
311 2023) who recommends to average all datapoints of one stroke of the TBM into one single value through an arithmetic
312 mean. If the stroke-wise averaging approach is chosen, this means that datapoints are averaged for every 1-2 meters. This
313 also has the advantage that the strokes are typically numbered, which eases the computation. However, other intervals
314 can be chosen as well and depending on the chosen method of discretization, the total number of datapoints reduces
315 again. After spatial discretization, data smoothing may be considered at this point by applying a moving average window
316 with reasonable width, where the window center is moved along the chainage and the values in the window are taken
317 into account. Oversmoothing (i.e. removing patterns in the data) through too large window sizes must be avoided,
318 therefore this measure has to be applied with care.

319 3.3. Parameter computation

320 After cleaning and discretizing the data, the parameter upon which the advance classification is to be based needs to be
321 computed. Even though the torque ratio is adopted as the exemplary parameter for advance classification in this study as
322 it is the one used in ÖNORM B 2203-2 (ÖNORM B 2203-2:2023, 2023), advance classification with other TBM parameters
323 is conceivable and it must be assessed for every construction site which parameter fits best. The specific excavation energy
324 after Teale (1965), for example, also correlates well with rock mass behavior in the authors' and others' experience
325 (Bergmeister and Reinhold 2017). Other parameters such as the specific penetration (Gong and Zhao 2009), the field

penetration index (FPI) (Delisio et al. 2013; Delisio and Zhao 2014; Hasanpour et al. 2014; Salimi et al. 2019) or the theoretical advance force (Heikal et al. 2021) can be considered as well.

3.4. Threshold definition and advance classification

The last step for TBM operational data based advance classification is to define one or several thresholds that discriminate one advance type from the others. Delisio and Zhao (2014), for example, define thresholds to identify different kinds of blocky rock mass behavior based on a modified version of the FPI, which is the inverse of the specific penetration.

In the ÖNORM B 2203-2, two different advance classes are differentiated:

- Regular advance is being registered when the following conditions are met: i) the excavated tunnel geometry fits the cutterhead geometry and there are no or only minor overbreaks; ii) the average torque ratio of a stroke lies within the project specific bounds; iii) the torque ratio is outside of these bounds but this is related to operational and logistical factors; iv) the shield friction is so low that it does not impact the performance (see Erharter et al. (2023) for more information on TBM shield friction); v) the cutters or other tools for the excavation are not violently damaged and there is no evidence of abnormal cutter wear; vi) only regular support measures and regular mucking is required.
- Exceptional advance is being registered if one or several of the criteria for regular advance are not fulfilled.

As can be seen, the ÖNORM B 2203-2 (2023) is not exclusively relying on the torque ratio as the decisive criteria to discriminate regular from exceptional advance and it is recommended to always consider if further criteria in addition to TBM operational data parameters are relevant.

Nevertheless, the focus of this work is advance classification based on the TBM data and thus the last step is to define thresholds. This can be done in different ways such as i) defining statistical thresholds that constitute the boundaries of advance classes (e.g. based on standard deviations). While this is a straightforward, understandable and transparent approach, it has limitations in advances that almost exclusively consist of one single class (i.e. almost exclusively regular advance or almost exclusively exceptional advance). ii) Another way of defining thresholds is to conjointly define a reference section of the tunnel where all parties agree that this was regular advance and then define the boundaries accordingly. (ÖNORM B 2203-2, 2023) This reference section of the tunnel should have a sufficiently representative length (ideally more than 100 meters) and consist of consecutive and complete strokes only.

Irrespective of the way the thresholds were determined, they should be regularly questioned and checked whether they are still fitting for the current excavation conditions and eventually updated. To account for different rock mass types throughout the excavation, different thresholds are possible in one tunnel excavation and consequently it might be necessary to define multiple reference sections for each threshold.

3.5. Exemplary processed TBM operational data

Figure 5 to Figure 7 show exemplary sections of the generated TBM datasets for TBM A, TBM B and TBM C. The data was first synthesized and postprocessed as described in section 2.2 and then processed as if it was real TBM operational data as described in the sections 3.1 to 3.4.

Standstills were removed as described in section 3.1 and datapoints with the same chainage were merged by computing the arithmetic mean of them. Spatial discretization (see section 3.2) was achieved by computing the arithmetic mean and the median of each single stroke for the parameters penetration, total advance force and cutterhead torque. In real advances, it is not necessary to use different ways of spatial discretization but here it was done to exemplify the effect on the final outcome of this seemingly minor difference (see below). The torque ratio as described in section 2.1 was then computed as the decisive parameter upon which the advance classification should be based. The parameters to compute the torque ratio for the exemplary datasets of this paper are given in Table 1.

Table 1: Input parameters to compute the torque ratio for the exemplary datasets of this paper.

Dataset	n cutters (n_{disc})	Disc cutter radius (R_{DC}) [mm]	Cutterhead diameter (D_{CH}) [m]	cutterhead torque at idle rotation (M_0) [kNm]
TBM A	50	241.3	7	180
TBM B	70	241.3	10	400
TBM C	60	241.3	9	220

Lastly, upper and lower thresholds to discriminate regular and exceptional advance were defined as described in section 3.4. The thresholds were set assuming that reference sections of regular advance were defined for the different datasets. The following thresholds were set for each dataset:

- TBM A: lower threshold: 0.35, upper threshold: 0.57
- TBM B: lower threshold: 0.45, upper threshold: 0.57
- TBM C: lower threshold: 0.53, upper threshold: 0.63

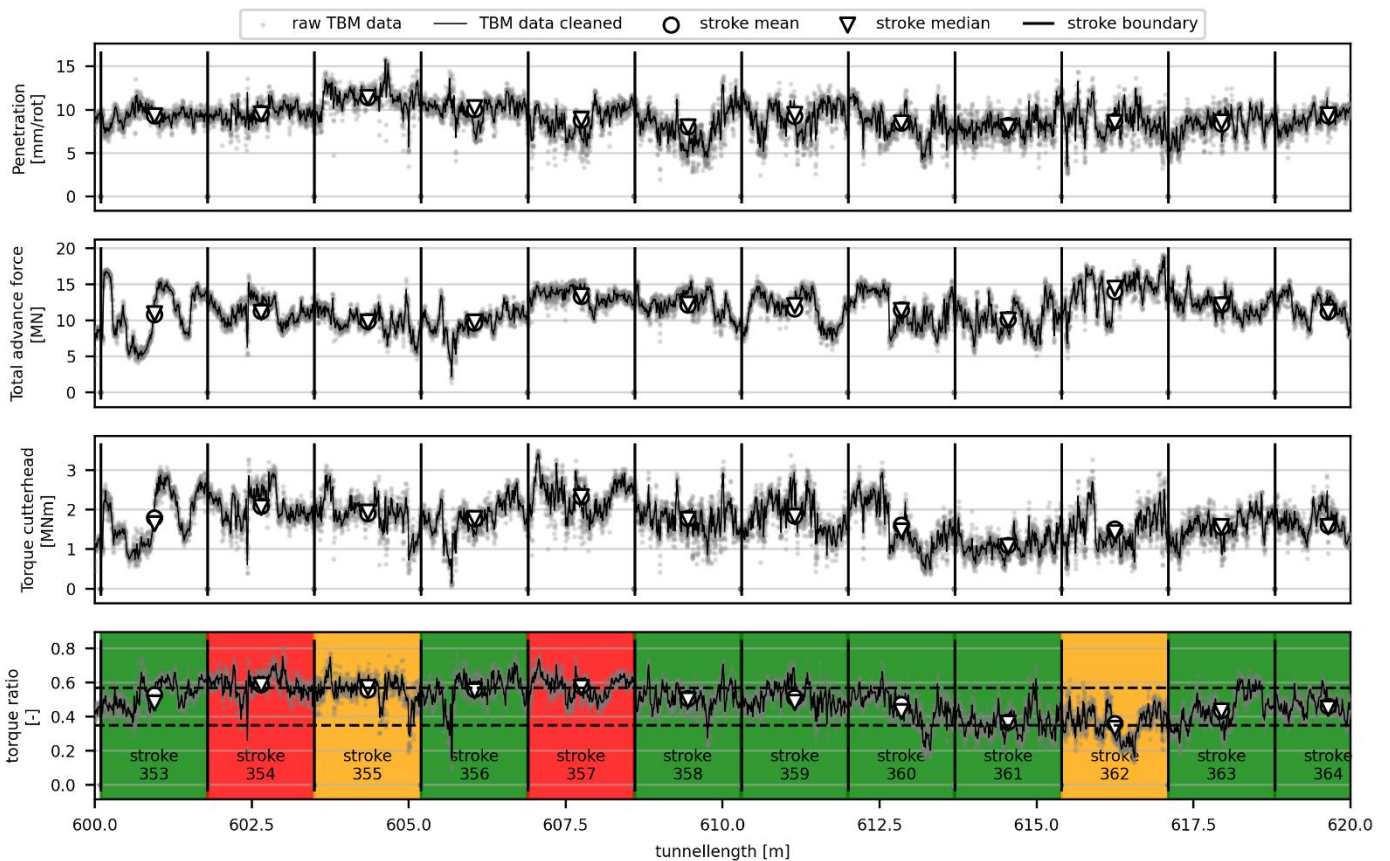
Note that all thresholds happen to be below 1 here, but in other excavations, especially upper thresholds > 1 are possible for the torque ratio as well. As given above, two ways of spatial discretization (i.e. arithmetic mean aggregation and median aggregation) were applied to exemplify the impact of different processing methods onto the final classification outcome. Given that and the defined thresholds, different lengths of regular- / exceptional advance were computed for the three different datasets (Table 2).

381 Table 2: Percentual lengths of advance classification for the three datasets and different spatial discretization methods.

Dataset	Regular / exceptional advance [%] (arithmetic mean)	Regular / exceptional advance [%] (median)
TBM A	80.3 / 19.7	78.8 / 21.2
TBM B	92.7 / 7.3	94.4 / 5.6
TBM C	83.4 / 16.6	79.6 / 20.4

382

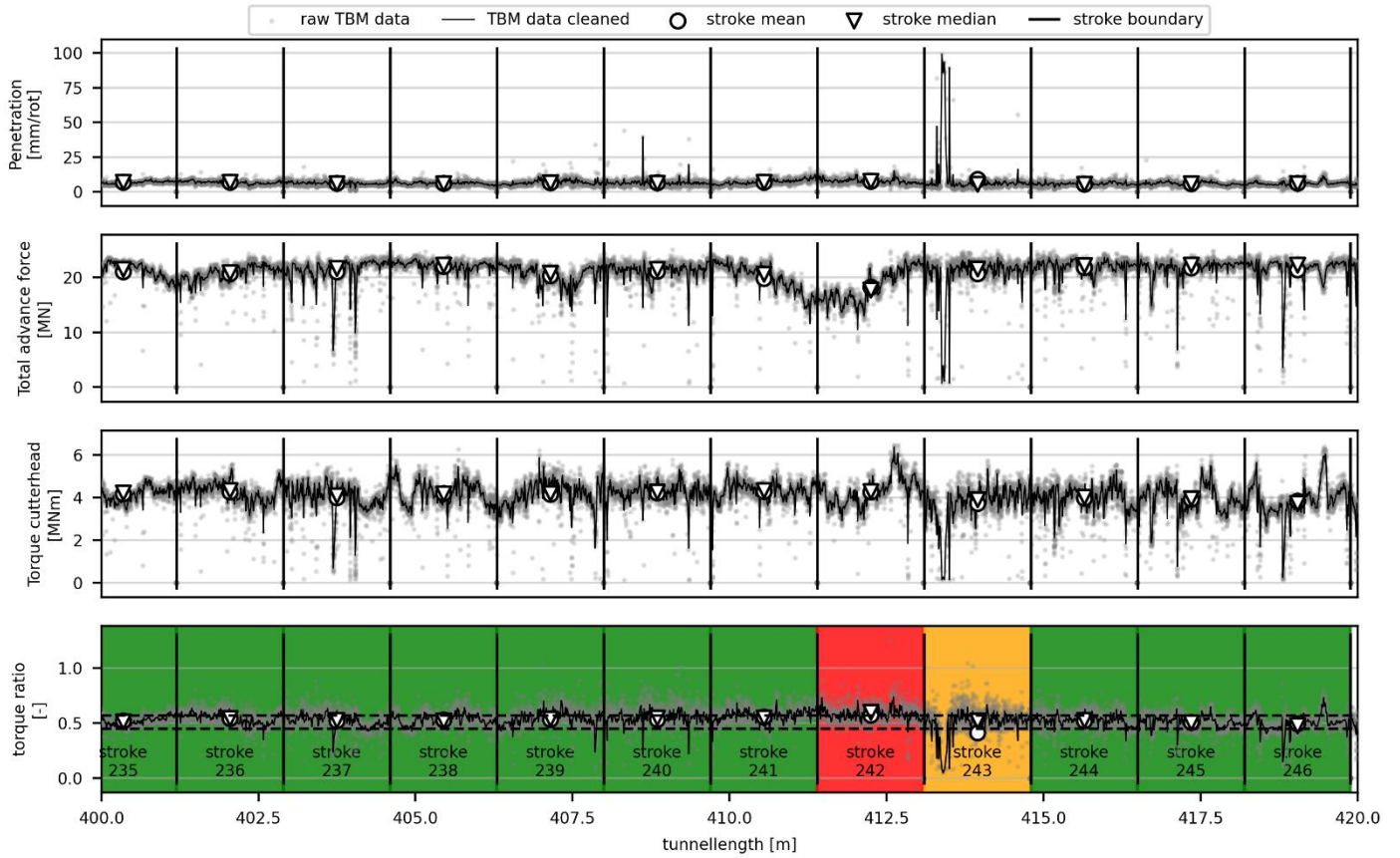
383 The fourth rows of Figure 5 to Figure 7 show the torque ratio based advance classification. Strokes where both the
 384 arithmetic mean- and the median-based torque ratio are within the specified thresholds or outside of the thresholds are
 385 marked in green and red respectively (i.e. green = regular advance, red = exceptional advance). In several strokes, however,
 386 either the arithmetic mean- or the median-based torque ratio were inside and outside of the defined boundaries and thus
 387 would lead to different classifications of that stroke (marked in orange). (see Github repository: data,
 388 "TBM_X_2_synthetic_strokes.xlsx" (replace X with A, B, C for each TBM), excel files)



389

390 Figure 5: TBM A: 30 meters of synthetic data based on a TBM excavation with an open gripper TBM where the machine was driven based on a constant
 391 penetration rate of 10 mm/rot. Explanation for colors in row 4 provided in the text.

Data Driven Advance Classification of Hard Rock TBMs
(non-peer reviewed preprint)



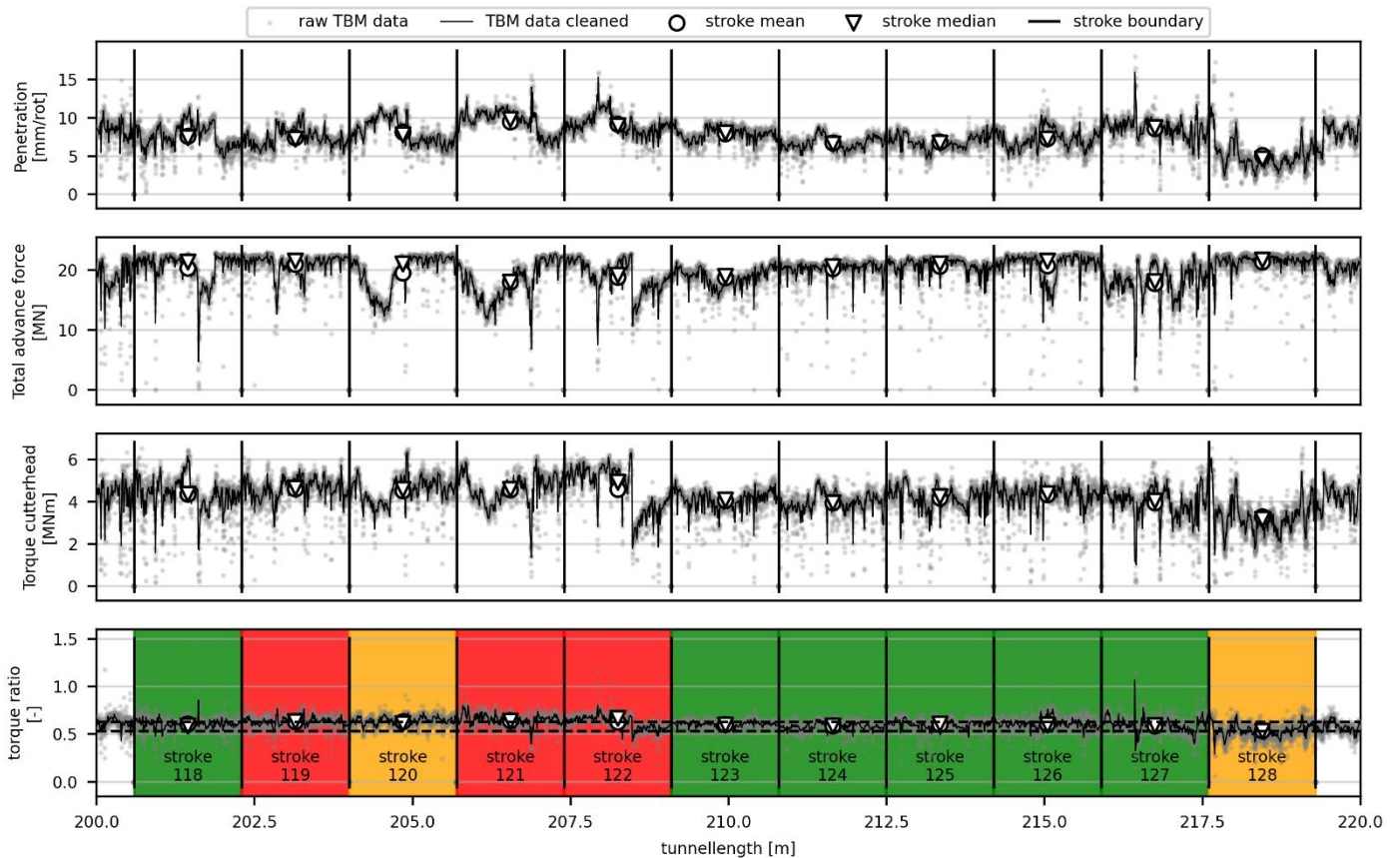
392

393

394

Figure 6: TBM B: 30 meters of synthetic data based on a TBM excavation with a double shield TBM. Explanation for colors in row 4 provided in the text.

Data Driven Advance Classification of Hard Rock TBMs
(non-peer reviewed preprint)



395

396

397

Figure 7: TBM C: 30 meters of synthetic data based on a TBM excavation with an open gripper TBM where the maximum advance force was limited to a bit over 20k MN. Explanation for colors in row 4 provided in the text.

398

4. Discussion

399

400

401

402

403

404

This paper addresses the opportunities and challenges of data-driven TBM advance classification, addressing practical guidance and emphasizing novel approaches. To overcome confidentiality restrictions often associated with TBM operational data, synthetic datasets were generated using generative adversarial networks. While these datasets realistically mimic TBM operational data, they lack some of the “noisiness” typical of real data. Despite this limitation, the datasets serve as valuable resources for training, education, and further research, providing the tunneling community with three 1-km open datasets for exploration and validation.

405

406

407

408

409

410

Section 3.5 demonstrated the computation of torque ratio-based classifications for these datasets and highlighted how minor variations in the data processing pipeline, such as differences in spatial discretization methods (mean vs. median), can significantly influence the classification outcomes. For example, the difference of 2-4% in the classification of “regular” versus “exceptional” advances might appear modest (Table 2) but could result in substantial cost variations for tunnels spanning several kilometers. Moreover, this discrepancy stems from a single processing change and additional changes or inconsistencies would further exacerbate classification divergences and complicate the identification of their root causes.

411

412

Despite affecting the absolute classification outcome, Figure 5 to Figure 7 also show how processing differences can lead to diverging assessments of individual sections of the tunnel (the orange colored strokes). While this effect might “average

413 out" over longer tunnel distances, it can lead to disputes and discussions on site if one way of processing classifies a specific
414 stroke as "regular" and another (slightly different) way classifies it as "exceptional". For example, in stroke 355 in Figure 5,
415 the median torque ratio would classify the stroke as exceptional advance while the arithmetic mean torque ratio would
416 classify it as regular. Given that stroke 354 was already exceptional and stroke 357 is also exceptional, this conflicting
417 assessment could lead to a dispute about the total length of this zone of exceptional advance. The same conflict potential
418 exists for the zone from stroke 119 to 122 in Figure 7, due to the different classifications of stroke 120.

419 The torque ratio has proven to be a reliable parameter for advance classification across various excavations. However, its
420 utility lies more in identifying relative changes and patterns than in its absolute value, which facilitates the detection of
421 irregular excavation conditions. Future work should refine the torque ratio's applicability by calibrating the assumed
422 tangential cutter force angle in a site- and TBM-specific manner, using detailed data and observations. Additionally,
423 operational indices such as FPI or specific energy could be incorporated to enhance the accuracy and reliability of torque
424 ratio-based classifications.

425 This study's novel contributions include the use of GANs to synthesize realistic TBM datasets and the exploration of data
426 processing sensitivities in advance classification. These findings provide actionable insights for geotechnical engineers,
427 helping bridge the gap between emerging data-driven methodologies and traditional tunneling practices while fostering
428 transparency and reproducibility in classification processes.

429 5. Conclusion and Outlook

430 Data analysis tools have become essential in mechanized tunneling to address complex ground conditions, larger tunnel
431 diameters, extended lengths, and increasing demands for improved performance and efficiency. TBM operations involve
432 numerous concurrent processes, monitored by hundreds of sensors recording data at intervals as short as one second.
433 Over the course of multi-year projects, these systems generate billions of data points, presenting challenges in storage
434 and analysis but also opportunities for more detailed operational insights.

435 Traditionally, tunneling data analysis has been retrospective, often used to evaluate ground conditions or address claims.
436 However, there is a growing shift towards real-time data analysis for continuous characterization and classification of TBM
437 system behavior. TBM operational data provides an uninterrupted record of tunneling conditions, offering valuable
438 parameters for understanding system behavior. For example, the Austrian standard ÖNORM B 2203-2 has introduced the
439 concept of "data-driven tunneling classification" into engineering practice, using parameters like the "torque ratio" to
440 distinguish between "regular" and "exceptional" advances.

441 This paper demonstrates how the torque ratio can be used to classify three TBM datasets, emphasizing its suitability for
442 identifying irregular tunneling and penetration conditions. It highlights that relative changes and patterns in the torque
443 ratio, rather than its absolute value, are critical for classification. However, setting appropriate thresholds and ensuring
444 methodological sensitivity remain significant challenges that can influence classification outcomes.

445 Data-driven advance classification offers clear advantages in providing objective and traceable results, enhancing accuracy
446 and reliability. Nonetheless, transparency in data processing is crucial to maintaining the integrity and trustworthiness of
447 the classification process and avoiding disputes.

448 This study also demonstrates the use of GANs to synthesize realistic operational data for TBM excavations. Future work
449 will focus on integrating geological and geotechnical data to develop geologically-coupled machine learning algorithms for
450 TBM operational data prediction. Such algorithms could forecast TBM operational data for new projects, enabling
451 performance and wear predictions based on realistic pre-project data. They could also support case studies on various
452 TBM types and allow efficient generation of samples for scenario analysis once models are trained. For projects with
453 reliable geological forecasts, synthetic data could facilitate early detection and response to unexpected geotechnical
454 conditions, thus further enhancing tunneling efficiency and risk management.

455 The following final recommendations are made for TBM operational data based advance classification:

- 456 ▪ A detailed step-by-step processing description needs to be established for every project and construction site where
457 TBM operational data based advance classification is to be done.
- 458 ▪ Script- / Code- based processing of the data should be used as it offers superior performance over spreadsheet
459 calculation software in dealing with large amounts of data and it ensures transparent processing.
- 460 ▪ The calculation basis needs to be made accessible to all involved parties via a version-controlled repository to facilitate
461 data driven decision making for the operation and financial management of the projects.

462 Additional work and analysis are underway to refine the process and make it more accessible to parties interested in this
463 approach and make the programs and data analysis process more efficient for practical applications.

464 [Data availability](#)

465 Exemplary generated TBM data and the code for the generation and analyses of the data can be found in the following
466 Github repository: https://github.com/geograz/TBM_advance_classification

467 [Funding statement](#)

468 Open Access publication funding by the Norwegian Geotechnical Institute is acknowledged.

469 [Declaration of Generative AI and AI-assisted technologies in the writing process](#)

470 During the preparation of this work the authors used ChatGPT from OpenAI (<https://openai.com/chatgpt/>) in order to
471 improve readability and language of the manuscript. After using this tool/service, the authors reviewed and edited the
472 content as needed and take full responsibility for the content of the publication.

473 [References](#)

474 Arjovsky M, Chintala S, Bottou L (2017) Wasserstein Generative Adversarial Networks. In: Precup D, Teh YW (eds)
475 Proceedings of the 34th International Conference on Machine Learning, vol 70. PMLR, pp 214–223

- 476 Asre S, Anwar A (2022) Synthetic Energy Data Generation Using Time Variant Generative Adversarial Network. Electronics
477 11:355. <https://doi.org/10.3390/electronics11030355>
- 478 Bach D, Holzer W, Leitner W, Radončić N (2018) The use of TBM process data as a normative basis of the contractual
479 advance classification for TBM advances in hard rock. Geomechanik und Tunnelbau 11:505–518.
480 <https://doi.org/10.1002/geot.201800042>
- 481 Bergmeister K, Reinhold C (2017) Learning and optimization from the exploratory tunnel - Brenner Base Tunnel.
482 Geomechanik und Tunnelbau 10:467–476. <https://doi.org/10.1002/geot.201700039>
- 483 Delisio A, Zhao J (2014) A new model for TBM performance prediction in blocky rock conditions. Tunnelling and
484 Underground Space Technology 43:440–452. <https://doi.org/10.1016/j.tust.2014.06.004>
- 485 Delisio A, Zhao J, Einstein HH (2013) Analysis and prediction of TBM performance in blocky rock conditions at the
486 Löttschberg Base Tunnel. Tunnelling and Underground Space Technology 33:131–142.
487 <https://doi.org/10.1016/j.tust.2012.06.015>
- 488 Erharter GH, Marcher T (2020) MSAC: Towards data driven system behavior classification for TBM tunneling. Tunnelling
489 and Underground Space Technology 103:103466. <https://doi.org/10.1016/j.tust.2020.103466>
- 490 Erharter GH, Marcher T (2021) On the pointlessness of machine learning based time delayed prediction of TBM operational
491 data. Automation in Construction 121:103443. <https://doi.org/10.1016/j.autcon.2020.103443>
- 492 Erharter GH, Goliash R, Marcher T (2023) On the Effect of Shield Friction in Hard Rock TBM Excavation. Rock Mech Rock
493 Eng. <https://doi.org/10.1007/s00603-022-03211-0>
- 494 Erharter GH, Bar N, Hansen TF, Jain S, Marcher T (2024) International Distribution and Development of Rock Mass
495 Classification: A Review. Rock Mech Rock Engng. <https://doi.org/10.1007/s00603-024-04215-8>
- 496 Farrokh E, Rostami J (2008) Correlation of tunnel convergence with TBM operational parameters and chip size in the
497 Ghomroud tunnel, Iran. Tunnelling and Underground Space Technology 23:700–710.
498 <https://doi.org/10.1016/j.tust.2008.01.005>
- 499 Farrokh E, Rostami J (2009) Effect of adverse geological condition on TBM operation in Ghomroud tunnel conveyance
500 project. Tunnelling and Underground Space Technology 24:436–446. <https://doi.org/10.1016/j.tust.2008.12.006>
- 501 Gong QM, Zhao J (2009) Development of a rock mass characteristics model for TBM penetration rate prediction.
502 International Journal of Rock Mechanics and Mining Sciences 46:8–18. <https://doi.org/10.1016/j.ijrmms.2008.03.003>
- 503 Goodfellow I, Pouget-Abadie J, Mirza M, Xu B, Warde-Farley D, Ozair S, Courville A, Bengio Y (2014) Generative Adversarial
504 Networks. In: Z. Ghahramani, M. Welling, C. Cortes, N. D. Lawrence, K. Q. Weinberger (eds) Advances in Neural
505 Information Processing Systems 27. Curran Associates, Inc, pp 2672–2680
- 506 Hasanpour R, Rostami J, Ünver B (2014) 3D finite difference model for simulation of double shield TBM tunneling in
507 squeezing grounds. Tunnelling and Underground Space Technology 40:109–126.
508 <https://doi.org/10.1016/j.tust.2013.09.012>
- 509 Hasanpour R, Rostami J, Barla G (2015) Impact of Advance Rate on Entrapment Risk of a Double-Shielded TBM in Squeezing
510 Ground. Rock Mech Rock Eng 48:1115–1130. <https://doi.org/10.1007/s00603-014-0645-2>

- 511 Hasanpour R, Rostami J, Schmitt J, Ozcelik Y, Sohrabian B (2020) Prediction of TBM jamming risk in squeezing grounds using
512 Bayesian and artificial neural networks. *Journal of Rock Mechanics and Geotechnical Engineering* 12:21–31.
513 <https://doi.org/10.1016/j.jrmge.2019.04.006>
- 514 Heikal G, Erharter GH, Marcher T (2021) A new parameter for TBM data analysis based on the experience of the Brenner
515 Base Tunnel excavation. *IOP Conf. Ser.: Earth Environ. Sci.* 833:12158. <https://doi.org/10.1088/1755-1315/833/1/012158>
- 516
- 517 Holzer W, Wagner OK, Leitner W (2021) Überarbeitung der österreichischen Werkvertragsnorm ÖNorm B 2203-2 für den
518 kontinuierlichen Vortrieb. *Geomechanics and Tunneling* 14:730–739. <https://doi.org/10.1002/geot.202100057>
- 519 Liu Q, Wang X, Huang X, Yin X (2020) Prediction model of rock mass class using classification and regression tree integrated
520 AdaBoost algorithm based on TBM driving data. *Tunnelling and Underground Space Technology* 106:103595.
521 <https://doi.org/10.1016/j.tust.2020.103595>
- 522 Liu Z, Li L, Fang X, Qi W, Shen J, Zhou H, Zhang Y (2021) Hard-rock tunnel lithology prediction with TBM construction big
523 data using a global-attention-mechanism-based LSTM network. *Automation in Construction* 125:103647.
524 <https://doi.org/10.1016/j.autcon.2021.103647>
- 525 Maidl B, Schmid L, Ritz W, Herrenknecht M (2008) *Hardrock tunnel boring machines*. Ernst, Berlin
- 526 Ng A, Jordan M (2001) On Discriminative vs. Generative Classifiers: A comparison of logistic regression and naive Bayes.
527 In: T. Dietterich, S. Becker, Z. Ghahramani (eds) *Advances in Neural Information Processing Systems*, vol 14. MIT Press
- 528 ÖGG (2023) Richtlinie Geotechnische Planung von Untertagebauten Zyklischer und kontinuierlicher Vortrieb:
529 Gebirgscharakterisierung und Vorgangsweise zur nachvollziehbaren Festlegung von bautechnischen Maßnahmen
530 während der Planung und Bauausführung
- 531 ÖNORM B 2203-2:2023 (2023) Untertagebauarbeiten ÖNORM B 2203-2:2023 03 01. Austrian Standards
- 532 Park N, Mohammadi M, Gorde K, Jajodia S, Park H, Kim Y (2018) Data synthesis based on generative adversarial networks.
533 *Proc. VLDB Endow.* 11:1071–1083. <https://doi.org/10.14778/3231751.3231757>
- 534 Pearson K (1901) LIII. On lines and planes of closest fit to systems of points in space. *The London, Edinburgh, and Dublin*
535 *Philosophical Magazine and Journal of Science* 2:559–572. <https://doi.org/10.1080/14786440109462720>
- 536 Radoncic N, Hein M, Moritz B (2014) Determination of the system behaviour based on data analysis of a hard rock shield
537 TBM / Analyse der Maschinenparameter zur Erfassung des Systemverhaltens beim Hartgesteins-Schildvortrieb.
538 *Geomechanik und Tunnelbau* 7:565–576. <https://doi.org/10.1002/geot.201400052>
- 539 Radončić N, Purrer W, Pichler K (2019) A model for fair compensation of construction costs in TBM tunneling: A novel
540 contribution. In: Peila D, Viggiani G, Celestino T (eds) *Tunnels and Underground Cities: Engineering and Innovation*
541 *meet Archaeology, Architecture and Art*. CRC Press, pp 4567–4573. <https://doi.org/10.1201/9780429424441-484>
- 542 Reinhold C, Schwarz C, Bergmeister K (2017) Development of holistic prognosis models using exploration techniques and
543 seismic prediction. *Geomechanik und Tunnelbau* 10:767–778. <https://doi.org/10.1002/geot.201700058>
- 544 Rostami J (1997) Development of a force estimation model for rock fragmentation with disc cutters through theoretical
545 modeling and physical measurement of crushed zone pressure. Dissertation, Colorado School of Mines

- 546 Rostami J (2013) Study of pressure distribution within the crushed zone in the contact area between rock and disc cutters.
547 International Journal of Rock Mechanics and Mining Sciences 57:172–186.
548 <https://doi.org/10.1016/j.ijrmms.2012.07.031>
- 549 Rostami J, Ozdemir L (1993) A New Model for Performance Prediction of Hard Rock TBMs. In: Bowerman LD (ed)
550 Proceedings / 1993 Rapid Excavation and Tunneling Conference, [1993 RETC], Boston, Massachusetts, June 13-17,
551 1993. Society for Mining Metallurgy and Exploration (SME) of the American Institute of Mining Metallurgical and
552 Petroleum Engineers, Littleton, Colo, pp 793–809
- 553 Salimi A, Rostami J, Moormann C (2019) Application of rock mass classification systems for performance estimation of rock
554 TBMs using regression tree and artificial intelligence algorithms. Tunnelling and Underground Space Technology
555 92:103046. <https://doi.org/10.1016/j.tust.2019.103046>
- 556 Teale R (1965) The concept of specific energy in rock drilling. International Journal of Rock Mechanics and Mining Sciences
557 & Geomechanics Abstracts 2:245. [https://doi.org/10.1016/0148-9062\(65\)90016-1](https://doi.org/10.1016/0148-9062(65)90016-1)
- 558 Thuro K (2002) Geologisch-felsmechanische Grundlagen der Gebirgslösung im Tunnelbau: Habilitationsschrift. In:
559 Münchner Geologische Hefte: Reihe B, pp 1–160
- 560 Unterlass PJ, Erharter GH, Marcher T (2022) Identifying Rock Loads on TBM Shields During Standstills (Non-Advance-
561 Periods). Geotech Geol Eng. <https://doi.org/10.1007/s10706-022-02263-x>
- 562 Unterlass PJ, Erharter GH, Saprionova A, Marcher T (2023) A WGAN Approach to Synthetic TBM Data Generation. In: Gomes
563 Correia A, Azenha M, Cruz PJS, Novais P, Pereira P (eds) Trends on Construction in the Digital Era, vol 306. Springer
564 International Publishing, Cham, pp 3–19. https://doi.org/10.1007/978-3-031-20241-4_1
- 565 van der Maaten L, Hinton G (2008) Visualizing Data using t-SNE. Journal of Machine Learning Research 9:2579–2605
- 566 Xue Y-D, Luo W, Chen L, Dong H-X, Shu L-S, Zhao L (2023) An intelligent method for TBM surrounding rock classification
567 based on time series segmentation of rock-machine interaction data. Tunnelling and Underground Space Technology
568 140:105317. <https://doi.org/10.1016/j.tust.2023.105317>
- 569 Zhang Q, Liu Z, Tan J (2019) Prediction of geological conditions for a tunnel boring machine using big operational data.
570 Automation in Construction 100:73–83. <https://doi.org/10.1016/j.autcon.2018.12.022>
- 571